Astronomy 61

Lab 4: Spectroscopy

Chua Zheng Fu Edrei
Department of Physics & Astronomy, Dartmouth College, Wilder Laboratory, Hanover, NH, USA

Dated: 22 February 2015

1 Purpose

The purpose of this lab is to reduce the raw spectrum data and to analyze the reduced spectrum of two stars (V*GY And and HD28123) and a quasar (B0624+6907) to determine their chemical compositions and to calculate their radial velocities using doppler shift.

Spectroscopy, in the context of Astronomy, is the process of splitting light from an astronomical source using (typically) a diffraction grating. The stellar spectrum will reveal the chemical composition of the source since the emission and absorption lines observed are unique to specific energy transition in a particular atom or molecule. For instance, hydrogen balmer lines correspond to energy transition to n=2 in hydrogen atom. $H\alpha$, which is the first line in the hydrogen balmer series (energy transition from n=3 to n=2), corresponds to a wavelength of 6562.82$\AA$. Stellar spectrum can also reveal the radial velocity of the astronomical source. By comparing the observed wavelength with the rest wavelength of an emission or absorption line, it is possible to calculate the radial velocity of the source using the doppler shift formula.

2 Finding Chart

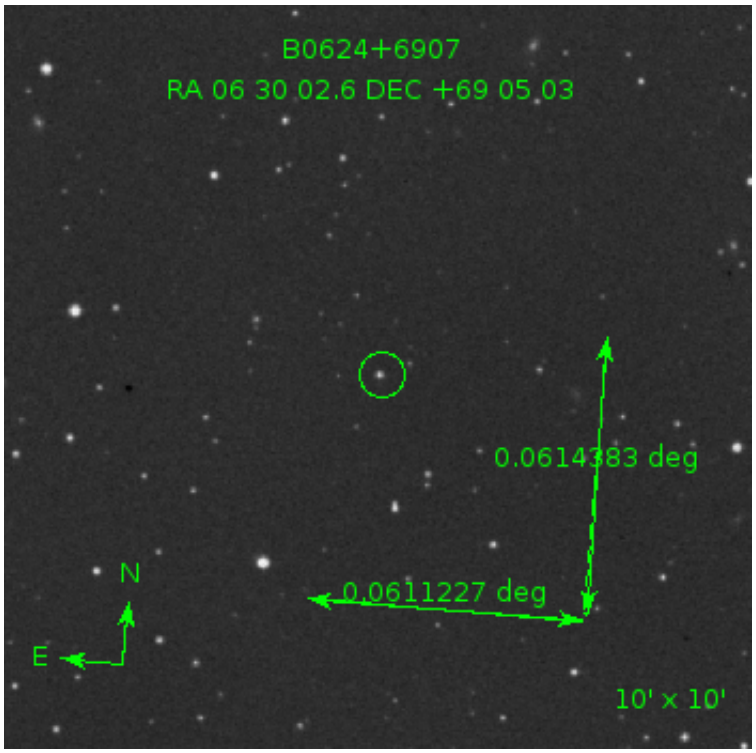

Fig. 1: Quasar B0624+6907 (RA:$06^h30^m02^s.6$ DEC $+69°05'03''$); dimension: 15' x 15'

As part of the lab, a finding chart for the quasar B0624+6907 was made. Fig. 1 shows the finding chart created using the Digitized Sky Survey (DSS) - STScI server. The dimension of the finding chart is 10 arcmins by 10 arcmins. The quasar was labelled with lines and annotated with its RA and DEC. A compass arrow gives directionality to the finding chart so that the observer using the chart can easily account for the orientation. A sense of the scale is also given by the double-arrows parallel to the north and east compass arrow.

3 Observing

John Thorstensen and Alexandros Zervos obtained the data used in this lab in 2013 October, using the Modular Spectrograph on the MDM 1.3 meter telescope. The spectrographs have been bias-subtracted and flatfielded. The observing log, which includes the filename, target name, type of observation, date and time of observation, airmass and exposure time, are presented in table 1 below.

Frame #	Target	Type	Date	Universal Time	Airmass	ExpTime(s)
hv050.fits	V*GY And	OBJECT	10/31/13	7:15:47	1.04	15
hv051.fits	V*GY And	OBJECT	10/31/13	7:19:42	1.05	15
hv052.fits	V*GY And	OBJECT	10/31/13	7:20:27	1.05	15
hv053.fits	V*GY And	OBJECT	10/31/13	7:21:12	1.05	15
hv252.fits	HgNe	COMPARISON	11/2/13	1:21:54	1.01	0.1
hv253.fits	Xe	COMPARISON	11/2/13	1:23:04	1.01	60
hv294.fits	HD28123	OBJECT	11/2/13	10:50:13	1.08	20
hv295.fits	HD28123	OBJECT	11/2/13	10:51:03	1.08	20
hv296.fits	B0624+6907	OBJECT	11/2/13	10:57:34	1.25	600
hv297.fits	B0624+6907	OBJECT	11/2/13	11:08:04	1.25	600

Table 1: Observation Log

4 Analysis

The spectrographs are analyzed using PyRAF. To obtain a calibrated one-dimensional spectra from the raw data, it is necessary to use the specred package in PyRAF, which can be accessed by typing *noao*, followed by *imred*, followed by *specred* in the command prompt.

Next, use the *apall* command to extract a 1-d spectra for the 2-d images. We performed this for the astronomical object, and not the comparison, first. The parameters for *apall* should be changed as follows: output format should be "multispec", default aperture should be -5 to +5, default background should be -50:-10,10:50, extraction paramter should be subtract the "fit", box car length is set to 1, weights are "variance", pfit is "fit1d", detect and replace bad pixels is "yes". Saturation level is 60000, readnoise is 8 and gain is 3. Perform this step for all the object frames (hv050, hv051, hv052, hv053, hv294, hv295, hv296 and hv297).

Then, use *imarith* to add the HgNe (hv252) and Xe (hv253) comparison images together. Extract the 1d spectra image of the combined comaprison image using *apall* as described above, but with the output format set as "onedspec" this time. The 1d spec for the comparison image will provide a baseline scale for the wavelength calibration for the object spectra. Fig. 2 shows the combined HgNe and Xe one dimensional spectra.

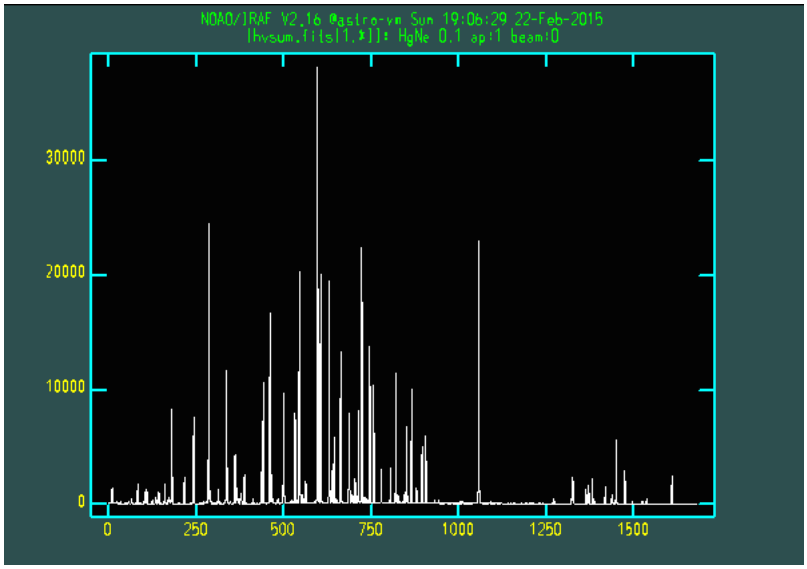

Fig. 2: Combined HgNe and Xe comparison one dimensional spectra

To convert the x-axis of the 1d spectra from pixels to wavelength, we made use of the fact that the comparison lines have accurately known wavelengths. By measuring the center of the line, it is possible to find the pixel co-ordinate x. To match the wavelength λ to the pixel co-ordinate x, we compare the spectrum lines with a labelled reference spectra (Fig. 3) to obtain several (x, λ) pairs. It should be noted that the one-dimensional comparison spectra (Fig. 2) is left-right inverted compared to the labelled reference spectra (Fig. 3).

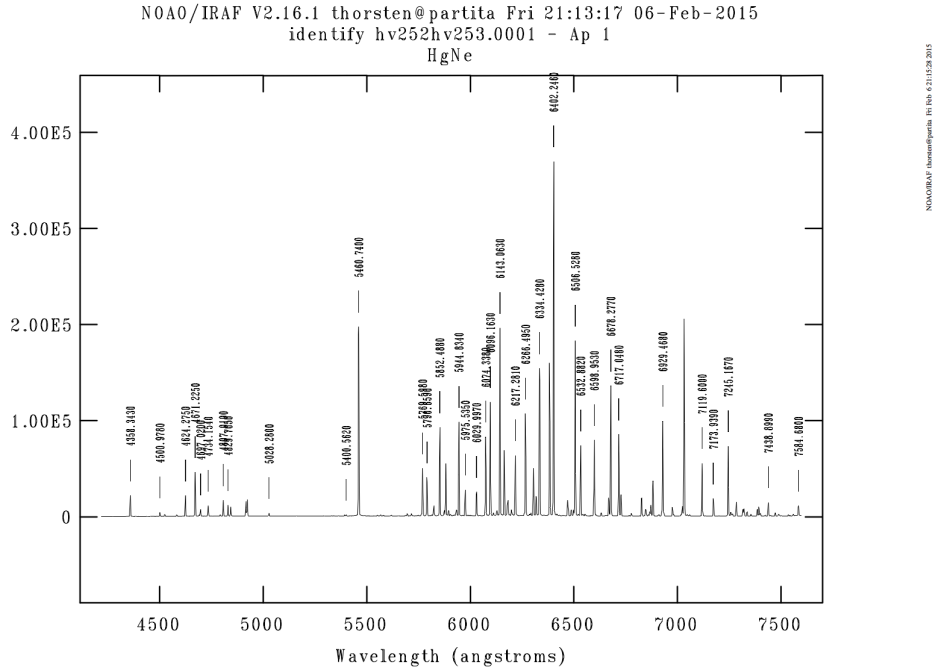

Fig. 3: Labelled reference one dimensional spectra

Following that, we use the *identify* command to measure the line centers and to obtain a polynomial fit to the (x, λ) pairs. We mark the pixel co-ordinate x on the combined spectra with its corresponding λ value using "m" on the *identify* command. We then prompt the program to create a sixth order legendre polynomial fit and to display the residues. The outliers are removed until the root-mean sqare error is below 0.1. We then proceed to save the wavelength solution and use *refspec* to match the wavelength scale to the object frames. After that, use *dispcor* to create the dispersion-corrected spectra.

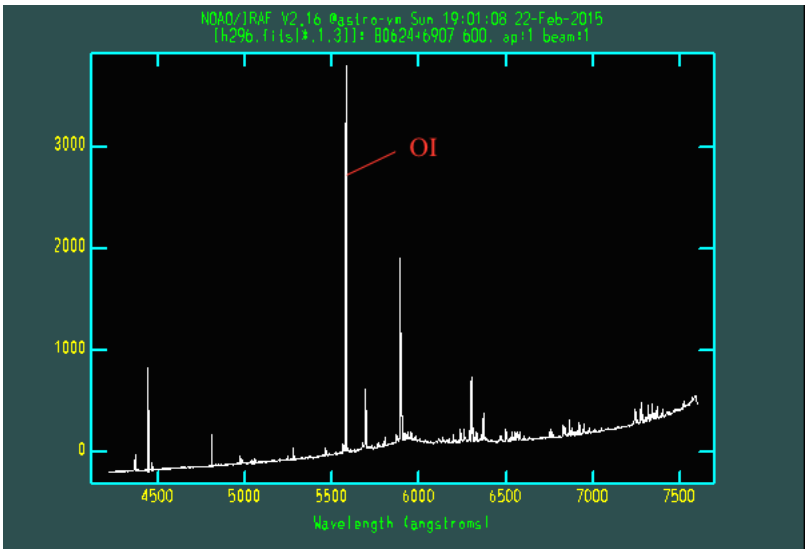

Fig. 4: Background spectra as displayed using splot for frame h296 (Quasar B0624+6907)

To test the wavelength solution, we used *splot* to dsiplay the background spectra that is subtracted from the object spectra (the third spectra in splot). Fig. 4 shows one of such spectrum. There should be a strong line in the background spectrum near $5577\mathring{A}$ that corresponds to neutral oxygen (OI) in the atmosphere. Expand the plot around the $5577\mathring{A}$ line by typing "a" with the cursor on either side of the line. Measure the wavelength by typing "k" with the cursor at the base on both side of the line to fit a gaussian curve. From the NIST Atomic Spectral lines database[1], it was determined that neutral oxygen has a wavelength of $5577.32\mathring{A}$.

Frame	$\lambda_{OI}(\mathring{A})$	$\delta_{scale}(\mathring{A})$
h50	5577.18	-0.16
h51	5577.35	0.01
h52	5577.28	-0.06
h53	5577.05	-0.29
h294	5578.53	1.19
h295	5578.33	0.99
h296	5577.98	0.64
h297	5577.86	0.52

Table 2: Error in converting pixel to wavelength for x-axis

Table 2 shows the wavelengths of neutral oxygen measured from the background spectrum of the object frames. It was noted that the wavelengths deviate from the actual wavelength by less than 0.03%, which suggest that the fit is very close. The small deviation from the actual wavelength, δ_{scale}, will introduce a systematic

[1]NIST Atomic Spectral Database. Retrieved from `http://physics.nist.gov/PhysRefData/ASD/lines_form.html`. Accessed on 23 February 2015

error later on in the measurement of spectral lines and the calculation of doppler shift. The systematic error due to error in fiting the scale to the object spectrum would be taken into account in future calculations.

Fig. 5, Fig. 6 and Fig. 7 show the calibrated one-dimensional spectra of V*GY, HD28123 and B0624+6907 respectively as obtained from the procedure outlined above. From the spectra, it is possible to identify certain wavelengths such as $H\alpha$ at 6562.82$\mathring{A}$ (identified in V*GY And and HD28123), $H\beta$ at 4861.33$\mathring{A}$ (identified in V*GY And, HD28123 and B0624+6907), $H\gamma$ at 4340.47$\mathring{A}$ (identified in V*GY And, HD28123 and B0624+6907), $H\delta$ at 4101.74$\mathring{A}$ (identified in B0624+6907) and $OIII$ at 5008.24$\mathring{A}$ (identified in B0624+6907). OII line at 6869.49$\mathring{A}$ is also observed for the spectra of V*GY And and HD28123.

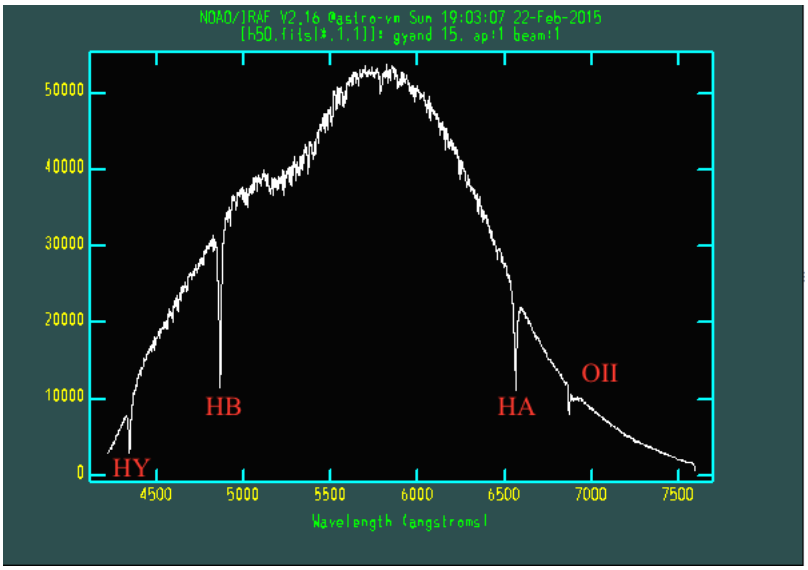

Fig. 5: Spectra of B9 star V*GY And (frame h50)

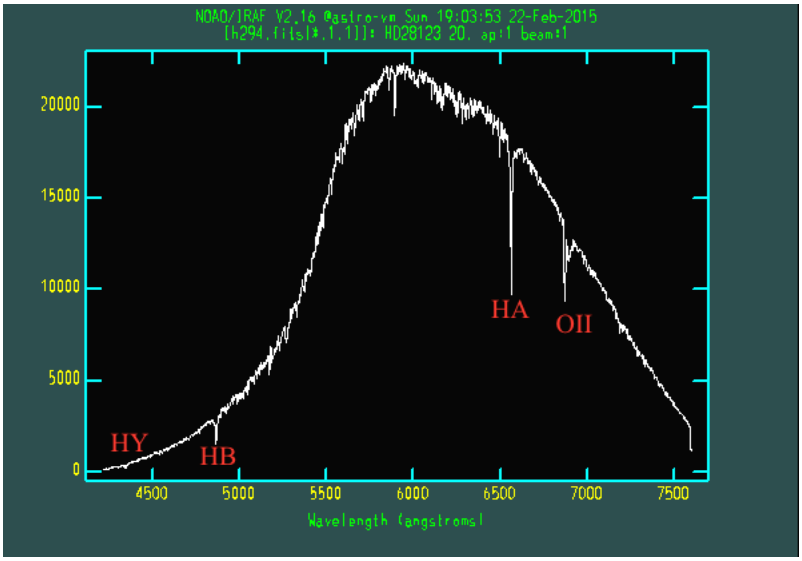

Fig. 6: Spectra of A0 star HD28123 (frame h294)

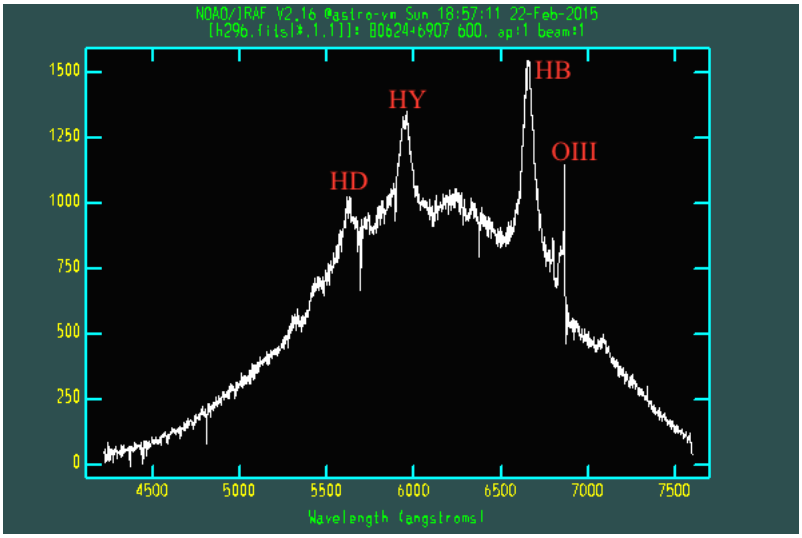

Fig. 7: Spectra of quasar (B0624+6907) (frame h296)

By measuring the observed wavelength and comparing with the rest wavelength of the same atomic spectra line in the lab, it is possible to calculate the radial velocity of the source using the doppler shift formula given below. The formula below assume non-relativistic speed. v is the radial velocity of the source with respect to Earth (positive value indicates that the source is moving away from Earth and negative value indicates that the sources is moving towards Earth), $\Delta\lambda$ is the change in wavelength ($\Delta\lambda = \lambda - \lambda_0$, where λ is the observed wavelength and λ_0 is the rest wavelength; therefore positive value indicates a redshift and negative value indicates a blue shift), λ_0 is the rest wavelength and c is the speed of light ($2.99792458 \times 10^5 km/s$).

$$v_{rad} = \frac{\Delta\lambda}{\lambda_0}c = \frac{\lambda - \lambda_0}{\lambda_0}c \tag{1}$$

We also need to take into account the systematic error introduced by the discrepancy in the matching of wavelength to pixel co-ordinate as mentioned above. To address this error, we subtract δ_{scale} as recorded in Table 2 from the change in wavelength $\Delta\lambda$ to get the corrected wavelength $\Delta\lambda_{corr}$. The corrected change in wavelength is then substituted into the doppler shift formula to find the radial velocity.

Finally, we also need to take into account the fact that the data were taken from Earth, which is a moving reference frame. Performing the measurement at different times of year would give a different radial velocity because the Earth's velocity changes direction as it goes around in orbit. To account for this, we use JSkyCalc to compute the barycentric correction (the correction is listed in Table 3 in the Results section). The barycentric correction is the velocity observed by an observer with the velocity of the barycenter, or ceter of mass of the solar system, which moves almost in a straight line at a constant speed.

We add the barycentric correction v_{bary} to the velocity calculated using the doppler shift formula to obtain the actual radial velocity. The revised formula is given below:

$$v_{rad} = \frac{\Delta\lambda_{corr}}{\lambda_0}c + v_{bary} = \frac{\Delta\lambda - \delta_{scale}}{\lambda_0}c + v_{bary} \tag{2}$$

The above steps to calculate radial velocity are repeated for a few distinct atomic spectra lines in each frame [$H\alpha$, $H\beta$ and $H\gamma$ for V*GY And (frame h50, h51, h52, h53) and HD28123 (frame h294, h295); $H\beta$, $H\gamma$, $H\delta$,

OIII for B0624+6907 (frame h296, h297)]. An average radial velocity is calculated for each frame based on the doppler shifts of the several spectra lines that are specified within each frame. Finally, an average radial velcoity is calculated for each object by averaging the radial velocities obtained for all the frames associated with that object.

To calculate the error in the radial velocity measured, we subtract the maximum radial velocity with the minimum radial velocity measured and divide it by two. This is shown in the formula below:

$$\sigma_v = \frac{v_{max} - v_{min}}{2} \tag{3}$$

The results discussed above are presented in Table 3 in the Results section.

5 Results

We identify $H\alpha$, $H\beta$ and $H\gamma$ to be the most prominent lines in the stellar spectrum for V*GY And and HD28123. The spectrum for both stars also contain the OII line at $6869.49\mathring{A}$ which is likely due to ionized oxygen in the Earth's atmosphere that is not subtracted from the spectrum. Based on the presence (dominance) and strength of the hydrogen balmer lines, and by comparing the stellar spectrum observed with a standard stellar spectra classification database (Jacoby et al 1984), we determined V*GY And to be a B type star and HD28123 to be an A type star. A cross-reference to the Simbad database reveals that V*GY And[2] is indeed a B9 type star and HD28123[3] is a A0 type star.

We calculate the radial velocities of V*GY And and HD28123 by measuring the doppler shifts of the $H\alpha$, $H\beta$ and $H\gamma$ lines. The procedure for extracting the radial velocity from the change in wavelength, and the method to account for the systematic error in matching wavelength to pixel co-ordinate and barycentric correction, are outlined in the Analysis section above. Table 3 presents the $H\alpha$, $H\beta$ and $H\gamma$ lines measured for each of the stellar frame (h50 - h53; h294 - h295), the barycentric correction value (V_{bary}), the corrected radial velocity calculated for each spectral line in every frame ($V_{H\alpha}$, $V_{H\beta}$ and $V_{H\gamma}$), and the average radial velocity calculated for each frame (V_{avg}).

Frame	$H\alpha(\mathring{A})$	$H\beta(\mathring{A})$	$H\gamma(\mathring{A})$	$H\Delta(\mathring{A})$	$OIII(\mathring{A})$	V_{bary} (km/s)	$V_{H\alpha}$ (km/s)	$V_{H\beta}$ (km/s)	$V_{H\gamma}$ (km/s)	$V_{H\Delta}$ (km/s)	V_{OIII} (km/s)	V_{avg} (km/s)
h50	6563.10	4860.85	4339.59	NA	NA	0.91	21.01	-18.82	-48.82	NA	NA	-15.54
h51	6562.18	4860.20	4338.83	NA	NA	0.90	-28.79	-69.40	-113.06	NA	NA	-70.42
h52	6561.71	4859.98	4338.73	NA	NA	0.90	-47.06	-78.65	-115.14	NA	NA	-80.28
h53	6561.82	4860.13	4339.15	NA	NA	0.90	-31.53	-55.22	-70.24	NA	NA	-52.33
h294	6562.92	4861.40	4339.13	NA	NA	14.57	-35.22	-54.50	-160.17	NA	NA	-83.30
h295	6563.10	4861.45	4340.31	NA	NA	14.56	-17.87	-39.09	-64.87	NA	NA	-40.61
h296	NA	6655.86	5948.92	5620.91	6864.77	16.76	NA	110529.89	111066.79	111004.74	111148.35	110937.44
h297	NA	6656.72	5949.94	5625.01	6864.64	16.75	NA	110590.30	111145.52	111313.17	111140.56	111047.39

Table 3: Observed wavelength and radial velocity measured from doppler shift from spectrum data

Table 4 presents the average radial velocity for V*GY And (by averaging the velocities measured in frame h50 - h53) and the average radial velocity for HD28123 (by averaging the velocities measured in frame h294 - h295). It also presents the associated error in the radial velocity (the method to calculate the error is presented in the analysis section). It should be noted that the radial velocity obtained from frame h50 using the $H\alpha$ line is an outlier; the radial velocity in frame h50 using the $H\alpha$ line suggests a red shift while all the other frames for the same star suggest a blue shift. Nevertheless, there is no evidence to suggest that the measurement for frame h50 is any less accurate that the measurement for the other frames since the author of the report did not

[2]Simbad - V*GY. Retrieved from `http://simbad.u-strasbg.fr/simbad/sim-id?Ident=V*GY+And&NbIdent=1&Radius=2&Radius.unit=arcmin&submit=submit+id`. Accessed on 21 February 2015

[3]Simbad - HD28123. Retrieved from `http://simbad.u-strasbg.fr/simbad/sim-basic?Ident=hd28123&submit=SIMBAD+search`. Accessed on 21 February 2015

conduct the experiment and has obtained the data from a third party. The radial velocity obtained with frame h50 is therefore retained in the calculation of the average radial velocity.

Target	V_{avg} (km/s)	σ_v (km/s)	% error
V*GY And	-54.64	68.07	124.57
HD28123	-61.96	71.15	114.84
B0624+6907	110992.41	154.21	0.14

Table 4: Radial velocity measured and error bar for V*GY And, HD28123 and B0624+6907

The radial velocity for V*GY And is given as $v_{rad} = -54.64 \pm 68.07 km/s$ and the radial velocity for HD28123 is given as $v_{rad} = -61.96 \pm 71.15 km/s$. It is noted that the percentage error in calculating the radial velocities are large and amount to 124.57% and 114.84% for V*GY And and HD28123 respectively.

The radial velocity for V*GY And is given as -0.3 km/s on the Simbad data base[4] while the radial velocity for HD28123 is not specified on Simbad. It can be noted that the average radial velocity measured using the spectrograph is very far off from the actual radial velocity as reported in the Simbad website despite the fact that the actual velocity still fall within the range of values measured. This is because the actual velocity is so small and the wavelength measured in *splot* is precise to only 2 decimal place. A $\Delta\lambda$ of $0.01\mathring{A}$ corresponds roughly to an uncertainty in velocity of 0.46 km/s. This results in large error bars. Potential experimental errors during observing that are unknown to the author of this report might have also contributed to the inaccuracy of the measured radial velocity.

The spectrum of the quasar B0624+6907 (h296 and h297) demanded separate treatment from the stellar spectrum of V*GY And and HD28123 because as Maarten Schmidt discovered in the 1960s, quasars can have very large redshifts. In fact, the redshifts are sometime large enough such that the spectral lines of the quasar can appear at wavelengths several times longer than the rest wavelength. Therefore, in order to identify the lines in the spectrum of the quasar to measure the redshift, we have to compare the quasar spectrum with a composite quasar spectrum as presented in scientific literature (Berk et al 2001). By comparing the patterns (based on the breadths and relative strengths of the lines) of the quasar spectrum with Fig 6 of the article published by Berk et al 2001, we determined four of the spectral lines to be $H\beta$ ($\lambda_0 = 4861.33\mathring{A}$), $H\gamma$ ($\lambda_0 = 4340.47\mathring{A}$), $H\delta$ ($\lambda_0 = 4101.74\mathring{A}$) and $OIII$ ($\lambda_0 = 5008.24\mathring{A}$). The radial velocities for frame h296 and h297 for the quasar are presented in Table 3. The procedure of obtaining the radial velocities are similar to the one for the stars.

It was noted that the redshifts, and thus the radial velocities, derived from the different individual lines deviate by less than 0.4%. The average redshift calculated is given as $z = 0.370 \pm 0.001$ while the average radial velcoity calculated is given as $v_{rad} = 110992.41 \pm 154.21 km/s$. This is approximately 37% the speed of light!

A comparison with the actual redshift as recorded in the Simbad data base (z = 0.374 in Simbad)[5] shows that our measured value agree closely with the actual value, with a deviation of approximately 1%.

$$v = Hd \tag{4}$$

Finally, we can use Hubble's law to estimate the distance of the quasar from the solar system. Hubble's law is given above, with v being the radial velocity in km/s, d is the distance of the quasar from the solar system in Mpc and H is Hubble's constant ($H \approx 72 kms^{-1}Mpc^{-1}$). It should be noted that with large redshifts,

[4]Simbad - V*GY. Retrieved from `http://simbad.u-strasbg.fr/simbad/sim-id?Ident=V*GY+And&NbIdent=1&Radius=2&Radius.unit=arcmin&submit=submit+id`. Accessed on 21 February 2015

[5]Simbad - B0624+6907. Retrieved from `http://simbad.u-strasbg.fr/simbad/sim-id?Ident=QSO+B0624\%2B6907`. Accessed on 21 February 2015

the concept of radial velocity becomes ambiguous. The redshift is mostly due to the expansion of the universe (expansion of spacetime itself) and is not the same thing as original speed.

Using Hubble's law, we determined that the quasar B0624+6907 is a distance $d = 1541.56 \pm 2.14 Mpc$ away from the solar system.

6 Summary

In this lab, we learnt to perform data reduction on raw spectroscopy data. From the reduced spectrographs, we analysed the chemical composition of V*GY And, HD28123 and quasar B0624+6907. We determined V*GY And to be a B9 type star and HD28123 to be an A0 type star based on the presence (dominance) and strength of their hydrogen balmer lines and by comparing it with a standard stellar spectra classification database.

We also learn to calculate the radial velocities of astronomical object based on the doppler shifts in their spectral lines. We measured the radial velocities of V*GY And to be $v_{rad} = -54.64 \pm 68.07 km/s$ and the radial velocity for HD28123 to be $v_{rad} = -61.96 \pm 71.15 km/s$. The large error bar is mainly due to the relatively small shifts in wavelength and the fact that the method to measure the wavelength is not very precise.

We also measure the redshift of the quasar B0624+6907 and show that $z = 0.370 \pm 0.001$. This is within 1% of the actual redshift of the quasar as recorded in the Simbad database. The velocity is calculated to be $v_{rad} = 110992.41 \pm 154.21 km/s$. Using the Hubble's relation, the distance of the quasar is determined to be $d = 1541.56 \pm 2.14 Mpc$ away from the solar system.

7 Acknowledgements

I would like to acknowledge professor John Thorstensen for providing the spectrum data for this lab and for outlining the instructions for reducing and analyzing the data. I have quoted his instructions extensively in the writing of the analysis section of this report. I am grateful to the TAs Erek Alper and Mackenzie Jones for helping with the analysis and result section of the lab. I have also collaborated with Natalia Drozdoff and Marie Schwalbe on the data reduction part of the lab.

8 References

Berk, D.V., Richards, G.T., Bauer, A. et al, 2001, AJ, 122, 555-557.

Jacoby, G.H., Hunter, D.A., Christian, C.A., 1984, ApJ, 56, 257-281.

NIST Atomic Spectral Database. Retrieved from `http://physics.nist.gov/PhysRefData/ASD/lines_form.html`. Accessed on 23 February 2015.

Simbad - B0624+6907. Retrieved from `http://simbad.u-strasbg.fr/simbad/sim-id?Ident=QSO+B0624\%2B6907`. Accessed on 21 February 2015.

Simbad - HD28123. Retrieved from `http://simbad.u-strasbg.fr/simbad/sim-basic?Ident=hd28123&submit=SIMBAD+search`. Accessed on 21 February 2015.

Simbad - V*GY. Retrieved from `http://simbad.u-strasbg.fr/simbad/sim-id?Ident=V*GY+And&NbIdent=1&Radius=2&Radius.unit=arcmin&submit=submit+id`. Accessed on 21 February 2015.

9 Appendix

Frame #	Target	Type	Date	Universal Time	Airmass	ExpTime(s)
hv050.fits	V*GY And	OBJECT	10/31/13	7:15:47	1.04	15
hv051.fits	V*GY And	OBJECT	10/31/13	7:19:42	1.05	15
hv052.fits	V*GY And	OBJECT	10/31/13	7:20:27	1.05	15
hv053.fits	V*GY And	OBJECT	10/31/13	7:21:12	1.05	15
hv252.fits	HgNe	COMPARISON	11/2/13	1:21:54	1.01	0.1
hv253.fits	Xe	COMPARISON	11/2/13	1:23:04	1.01	60
hv294.fits	HD28123	OBJECT	11/2/13	10:50:13	1.08	20
hv295.fits	HD28123	OBJECT	11/2/13	10:51:03	1.08	20
hv296.fits	B0624+6907	OBJECT	11/2/13	10:57:34	1.25	600
hv297.fits	B0624+6907	OBJECT	11/2/13	11:08:04	1.25	600

Table 5: Observation Log